Eur. Phys. J. A 4, 251–258 (1999)

THE EUROPEAN
PHYSICAL JOURNAL A

The spin and flavour dependence of high-energy photoabsorption

S.D. Bass[1,2,a], M.M. Brisudová[3,b]

[1] Institut für Theoretische Kernphysik, Universität Bonn, Nussallee 14–16, D-53115 Bonn, Germany
[2] Max Planck Institut für Kernphysik, Postfach 103980, D-69029 Heidelberg, Germany
[3] Theoretical Division, Los Alamos National Laboratory, Los Alamos, NM 87545, USA

Received: 23 October 1998
Communicated by W. Weise

Abstract. We analyse the low x, low Q^2 polarised photoabsorption data from SLAC and use this data to make a first estimate of the high-energy part of the Drell-Hearn-Gerasimov sum-rule. The present status of spin dependent Regge theory is discussed.

PACS. 11.55.Hx Sum rules – 12.40.Nn Regge theory, duality, absorptive/optical models – 13.60.Hb Total and inclusive cross sections (including deep inelastic processes) – 13.88.+e Polarization in interactions and scattering

1 Introduction

The Drell-Hearn-Gerasimov sum-rule [1] for spin dependent photoproduction and the Bjorken [2] and Ellis-Jaffe [3] sum-rules for polarised deep inelastic scattering provide important constraints for our understanding of the internal spin structure of the nucleon.

Consider polarised $\gamma - N$ scattering where σ_A and σ_P denote the two cross-sections for the absorption of a transversely polarised photon with spin anti-parallel σ_A and parallel σ_P to the spin of the target nucleon. We let q_μ and p_μ denote the momentum of the incident photon and target nucleon and define $Q^2 = -q^2$ and $\nu = p.q/m$ where m is the nucleon mass. The spin dependent part of the total γN cross-section is

$$(\sigma_A - \sigma_P) = \frac{4\pi\alpha^2}{m\mathcal{F}}(g_1 - \frac{Q^2}{\nu^2} g_2). \qquad (1)$$

Here g_1 and g_2 are the nucleon's first and second spin dependent structure functions and $\mathcal{F}$ is the photon flux factor.

For real photons, $Q^2 = 0$, the Drell-Hearn-Gerasimov sum-rule [1] (for reviews, see [4,5]) relates $(\sigma_A - \sigma_P)$ to the square of the nucleon's anomalous magnetic moment κ:

$$\text{(DHG)} \equiv -\frac{4\pi^2\alpha\kappa^2}{2m^2} = \int_{\nu_{th}}^{\infty} \frac{d\nu}{\nu}(\sigma_A - \sigma_P)(\nu). \qquad (2)$$

In deep inelastic scattering ($Q^2 \to \infty$) the light-cone operator product expansion relates the first moment of the structure function g_1 to the scale-invariant axial charges of the target nucleon by [6,7]

$$\int_0^1 dx\ g_1^p(x,Q^2)$$
$$= \left(\frac{1}{12} g_A^{(3)} + \frac{1}{36} g_A^{(8)}\right)\Big\{1 + \sum_{\ell\geq 1} c_{\mathrm{NS}\ell}\, \alpha_s^\ell(Q)\Big\}$$
$$+ \frac{1}{9} g_A^{(0)}|_{\mathrm{inv}}\Big\{1 + \sum_{\ell\geq 1} c_{\mathrm{S}\ell}\, \alpha_s^\ell(Q)\Big\} + \mathcal{O}(\frac{1}{Q^2}). \qquad (3)$$

Here $g_A^{(3)}$, $g_A^{(8)}$ and $g_A^{(0)}|_{\mathrm{inv}}$ are the isotriplet, SU(3) octet and scale-invariant flavour-singlet axial charges respectively. The flavour non-singlet $c_{\mathrm{NS}\ell}$ and singlet $c_{\mathrm{S}\ell}$ coefficients are calculable in ℓ-loop perturbation theory and have been calculated to $O(\alpha_s^3)$ precision [7].

The Bjorken sum-rule [2] for the isovector part of $\int_0^1 dx g_1$ has been verified to 10% accuracy in polarised deep inelastic scattering experiments at CERN [8,9], DESY [10] and SLAC [11,12]. These experiments have also revealed a four standard deviations violation of OZI in the flavour singlet axial charge $g_A^{(0)}|_{\mathrm{inv}}$ prompting many theoretical ideas about the internal spin structure of the nucleon — for recent reviews see [13].

At the present time, there are no direct measurements of $(\sigma_A - \sigma_P)$ at $Q^2 = 0$. Polarised real photon beam experiments are planned or presently underway at the CEBAF, ELSA, GRAAL, LEGS and MAMI facilities to investigate the spin structure of the nucleon at $Q^2 = 0$ with photon energies up to 6 GeV (or $\sqrt{s_{\gamma p}} \simeq 3.5$GeV). These experiments will measure the low and intermediate energy contributions to the Drell-Hearn-Gerasimov sum-rule.

[a] Steven.Bass@mpi-hd.mpg.de
[b] brisuda@t5.lanl.gov

As we prepare for these experiments it is helpful to have some guide what to expect. Multipole analyses [14] of (unpolarised) pion photoproduction data suggest that the isosinglet part of the Drell-Hearn-Gerasimov sum-rule (-219μb) may be nearly saturated by nucleon resonance contributions with estimates ranging between -225μb and -222μb. In contrast, multipole estimates of nucleon resonance contributions to the isovector part of the DHG integral (+15μb) range between -65μb and -39μb — that is, different in sign and a factor of 2-4 bigger than the theoretical prediction for the isovector part of the fully inclusive sum-rule. The nucleon resonance contributions to (DHG) seem to saturate by $\nu = 1.2$GeV ($\sqrt{s_{\gamma p}} = 1.8$GeV).

The present programme of polarised photoproduction experiments will measure the nucleon resonance contributions to (DHG). They will also measure contributions from non-resonant vector-meson-dominance [15] and strangeness production in the final state [4,16].

High-energy polarised real-photon beams would allow this programme to be extended into the Regge region and to make contact with deep inelastic measurements of g_1 at small Bjorken x. Possible experimental options include an upgraded 25GeV CEBAF machine ($\sqrt{s_{\gamma p}} \simeq 7$GeV) and a polarised proton beam at HERA ($\sqrt{s_{\gamma p}} \simeq 50 - 250$GeV).

Motivated by these experiments we make a first estimate of the high-energy part of the Drell-Hearn-Gerasimov sum-rule. We start in Sects. 2 and 3 with a phenomenological overview of spin dependent Regge theory and the present status of high-energy photoabsorption data from $Q^2 \simeq 0.25\text{GeV}^2$ through to polarised deep inelastic scattering. In Sect. 4 we analyse the SLAC data on g_1 at low x and low Q^2 and use this data to estimate the high-energy part of the Drell-Hearn-Gerasimov sum-rule. We estimate that about 10% of the total Drell-Hearn-Gerasimov integral may come from large $\sqrt{s_{\gamma p}}$ (greater than 2.5GeV). This high-energy contribution is predominantly isotriplet. Finally, in Sect. 5, we make our conclusions.

2 g_1 at large $\sqrt{s_{\gamma p}}$

Regge theory makes a prediction for the large $s_{\gamma p}$ ($= (p+q)^2$) dependence of the spin dependent total photoproduction ($Q^2 = 0$) cross-sections. It is often used to describe the small x behaviour of deep inelastic structure functions (Q^2 larger than about 2GeV^2).

The Regge prediction for the isovector part of $(\sigma_A - \sigma_P)$ is [17]:

$$\left(\sigma_A - \sigma_P\right)^{(p-n)} \sim s^{\alpha_{a_1}-1}, \quad (Q^2 = 0,\ s_{\gamma p} \to \infty). \quad (4)$$

Here, α_{a_1} is the intercept of the isovector $a_1(1260)$ Regge trajectory. If one makes the usual assumption that the a_1 trajectory is a straight line running parallel to the (ρ, ω) trajectories, then one finds $\alpha_{a_1} = -0.4$. This value lies within the phenomenological range $(-0.5 \leq \alpha_{a_1} \leq 0)$ quoted by Ellis and Karliner [18].

For the isoscalar part of $(\sigma_A - \sigma_P)$, Regge theory predicts [17,19,20]:

$$\left(\sigma_A - \sigma_P\right)^{(p+n)} \sim N_0 s^{\alpha_{f_1}-1} + N_g \frac{\ln\frac{s}{\mu^2}}{s} + N_{PP} \frac{1}{\ln^2 \frac{s}{\mu^2}},$$
$$(Q^2 = 0,\ s_{\gamma p} \to \infty). \quad (5)$$

Here, α_{f_1} is the intercept of the isoscalar $f_1(1285)$ and $f_1(1420)$ Regge trajectories – expected to be $\alpha_{f_1} \simeq -0.5$. The logarithm terms in (5) are associated with possible gluonic exchanges in the t-channel. The $\ln s/s$ term is induced by any vector short-range exchange-potential [19] — for example, two non-perturbative gluon exchange in the Landshoff-Nachtmann model of the soft pomeron [21] — and the $1/\ln^2 s$ term represents any two-pomeron cut contribution [20]. The mass parameter μ is taken as a typical hadronic scale (between 0.2 and 1.0GeV); the normalisation factors N_0, N_g and N_{PP} in (5) are to be determined from experiment. Each of the possible Regge contributions in (4,5) yield a convergent Drell-Hearn-Gerasimov integral (2).

It is an open question how far one can increase Q^2 and still trust soft Regge theory to provide an accurate description of $(\sigma_A - \sigma_P)$. If one assumes that α_{a_1} is independent of Q^2, then one expects [17,18] the isovector part of g_1 to exhibit the small x behaviour:

$$g_1^{(p-n)} \sim x^{-\alpha_{a_1}}, \quad (x \to 0\ ,\ \forall Q^2). \quad (6)$$

(Here, $g_1^{(p-n)} = (g_1^p - g_1^n)$.) High-energy, polarised photoabsorption data presently exist from $Q^2 \simeq 0.25\text{GeV}^2$ through to polarised deep inelastic scattering. We discuss this data below. In Sect. 3 we concentrate on g_1 at small x and deep inelastic Q^2 (where the data is most accurate). We discuss the possible Q^2 dependence of high-energy photoabsorption in the transition region between photoproduction and deep inelastic scattering. In Sect. 4 we consider the low x, low Q^2 data from SLAC and SMC.

3 Deep inelastic measurements of g_1 at small x

Polarised deep inelastic data consistently indicate a strong isotriplet term in g_1 which rises at small x. The SLAC measurements of g_1 have the smallest experimental error in the x range $(0.01 < x < 0.12)$.

In Fig. 1 we show the SLAC data[1] on the isovector $g_1^{(p-n)}$ and isoscalar $g_1^{(p+n)}$ $(= g_1^p + g_1^n)$ parts of g_1. We find good fits to this data:

$$g_1^{(p-n)} \sim (0.13) x^{-0.49} \text{ at } (0.01 < x < 0.12) \quad (7)$$

[1] Our data set consists of the E-154 neutron data evolved to $Q^2 = 5\text{GeV}^2$ [12] and the E-143 proton data ($Q^2 = 3\text{GeV}^2$) [11] together with the preliminary E-155 proton data points at $x = (0.016, 0.024)$ and $Q^2 = 5\text{GeV}^2$ [22]. Following Soffer and Teryaev [23] we combine this E-143, E-154 and E-155 data as if they were taken at the same Q^2. The theoretical error induced by this procedure is of the order of 10%; it is small compared to the present experimental error on the data

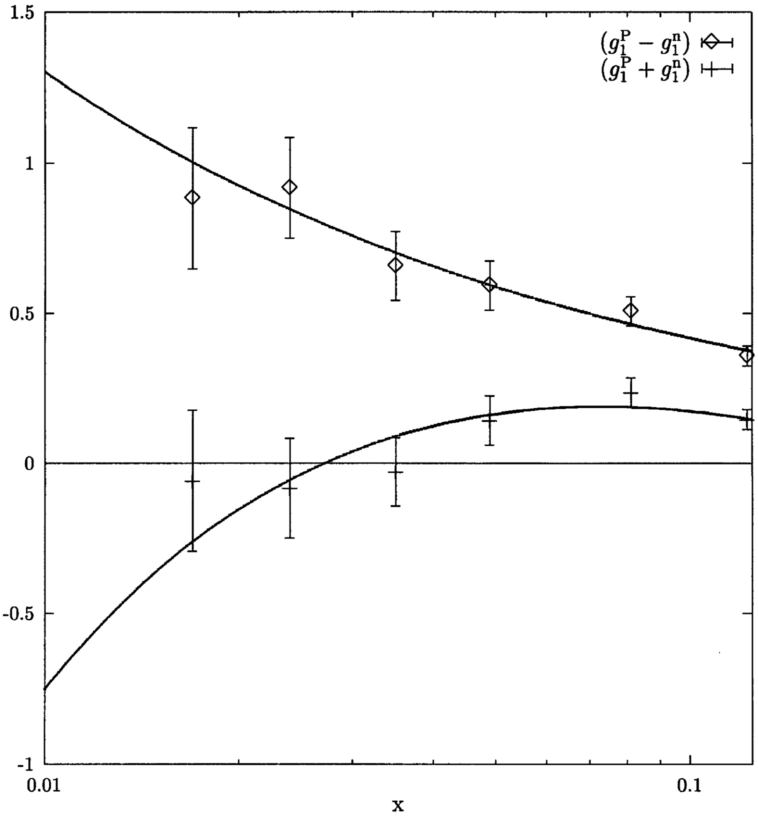

Fig. 1. The SLAC data on g_1. The upper curve shows the fit (12) to the isotriplet $g_1^{(p-n)}(x)$. The lower curve shows the fit (13) to the isosinglet $g_1^{(p+n)}(x)$ at $Q^2 \simeq 4\mathrm{GeV}^2$

and

$$g_1^{(p+n)} \sim -(0.23)x^{-0.56} + (0.28)(2\ln\frac{1}{x} - 1)$$
$$\text{at } (0.01 < x < 0.12) \quad (8)$$

with χ^2 =2.19 and 2.95 respectively (each for 6 degrees of freedom). The functional form $(2\ln\frac{1}{x} - 1)$ is taken from the two non-perturbative gluon exchange model [21]. We obtain a better fit to $g_1^{(p+n)}$ by including it than if we use only a simple power term; in the latter case we obtain a best fit $g_1^{(p+n)} \sim (0.35)x^{+0.36}$ with larger χ^2 (=7.1 for 6 d.o.f.).

There are several important properties of this data.

The isosinglet $g_1^{(p+n)}$ is small and consistent with zero in the measured small x range $(0.01 < x < 0.05)$. Polarised gluon models [24] predict that $g_1^{(p+n)}$ may become strongly negative at smaller values of x ($\sim 10^{-4}$) but this remains to be checked experimentally.

The magnitude of $g_1^{(p-n)}$ is significantly greater than the magnitude of $g_1^{(p+n)}$ in the measured small x region. This is in contrast to unpolarised deep inelastic scattering where the small x region is dominated by isoscalar pomeron exchange.

If Regge theory is describing the g_1 data at small x, then we find $\alpha_{a_1} = +\frac{1}{2}$ — that is, roughly equal in magnitude but opposite in sign to the Regge prediction. At first glance, this result is surprising since Regge theory provides a good description of the NMC measurements of both the isotriplet and isosinglet parts of F_2 in the same small x range $(0.01 < x < 0.1)$ at $Q^2 \simeq 5\mathrm{GeV}^2$.

In practice, the shape of g_1 at small x is Q^2 dependent. The Q^2 dependence is driven by DGLAP evolution and, at very small x ($\sim 10^{-3}$), by the resummation of $\alpha_s^l \ln^{2l} x$ radiative corrections — see eg. [25]. Next-to-leading order QCD analyses of polarised deep inelastic data have been carried out in [24,26–28]. In the rest of this section we outline the important features of QCD evolution for the shape of $g_1^{(p-n)}$ at small x. We also make some phenomenological observations comparing the small x behaviour of $g_1^{(p-n)}$ with the small x behaviour of the unpolarised structure function $F_2^{(p-n)}/2x$.

3.1 Q^2 dependence

We define an effective intercept $\tilde{\alpha}_{a_1}(Q^2)$ to describe the small x behaviour of g_1 at finite Q^2: $g_1^{(p-n)} \sim x^{-\tilde{\alpha}_{a_1}}$. The net Q^2 dependence of $\tilde{\alpha}_{a_1}$ depends strongly on the value of $\tilde{\alpha}_{a_1}$ which is needed to describe the leading twist part of $g_1^{(p-n)}$ at low momentum scales — for example $\mu_0^2 \sim 0.3\mathrm{GeV}^2$. Let $(\Delta u - \Delta d)(x)$ denote the leading twist (=2) part of $g_1^{(p-n)}$. DGLAP evolution of $(\Delta u - \Delta d)(x)$ from μ_0^2 to deep inelastic Q^2 shifts the weight of the distribution from larger to smaller values of x whilst keeping the area under the curve, $g_A^{(3)}$, constant. QCD evolution has the practical effect of “filling up” the small x region –

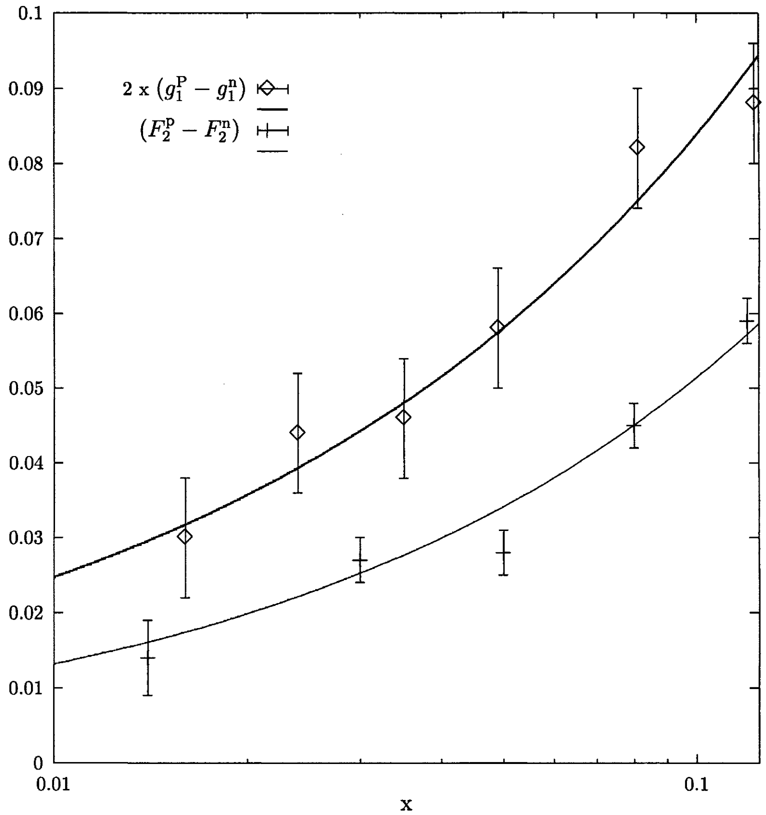

Fig. 2. Comparison of the isotriplet parts of the polarised $2xg_1$ (SLAC) and unpolarised F_2 (NMC) at $Q^2 \simeq 4\text{GeV}^2$

increasing the value of $\tilde{\alpha}_{a_1}$ with increasing Q^2. The scale independence of $g_A^{(3)}$ provides an important constraint on the change in $\tilde{\alpha}_{a_1}$ under QCD evolution. The closer that $\tilde{\alpha}_{a_1}(\mu_0^2)$ is to the Regge prediction -0.4, the more that $\tilde{\alpha}_{a_1}(Q^2)$ will grow in order to preserve the area under $(\Delta u - \Delta d)(x)$ when we increase Q^2 to values typical of deep inelastic scattering.

Badelek and Kwiecinski [29] have investigated the effect of DGLAP and $\alpha_s \ln^2 x$ resummation on the small x behaviour of $g_1^{(p-n)}$. They find a good fit to the data using a flat small-x input distribution at $Q_0^2 = 1\text{GeV}^2$. In their optimal NLO QCD fit to polarised deep inelastic data Glück, Reya, Stratmann and Vogelsang [27] used a rising input at $\mu_0^2 \simeq 0.3\text{GeV}^2$.

Whilst QCD evolution offers a possible explanation of the rise in $g_1^{(p-n)}$ at small x in deep inelastic scattering, it does not well constrain the value of $\tilde{\alpha}_{a_1}$ at low Q^2. In order to resolve the Q^2 dependence of $\tilde{\alpha}_{a_1}$ it would be helpful to have an accurate measurement of the small x behaviour of $g_1^{(p-n)}$ as a function of Q^2 in the transition region between photoproduction and deep inelastic scattering. In the rest of this paper we take $\alpha_{a_1} = \tilde{\alpha}_{a_1}(Q^2 = 0)$ as a free parameter between $-\frac{1}{2}$ and $+\frac{1}{2}$.

3.2 Comparison of $(g_1^p - g_1^n)$ and $(F_2^p - F_2^n)$

It is interesting to compare the isotriplet part of g_1 with the isotriplet part of F_2 (the nucleon's spin independent structure function). In the QCD parton model

$$2x(g_1^p - g_1^n) = \frac{1}{3}x\left[(u+\overline{u})^{\uparrow} - (u+\overline{u})^{\downarrow} - (d+\overline{d})^{\uparrow} + (d+\overline{d})^{\downarrow}\right] \otimes \Delta C_{NS} \tag{9}$$

and

$$(F_2^p - F_2^n) = \frac{1}{3}x\left[(u+\overline{u})^{\uparrow} + (u+\overline{u})^{\downarrow} - (d+\overline{d})^{\uparrow} - (d+\overline{d})^{\downarrow}\right] \otimes C_{NS}. \tag{10}$$

Here u and d denote the up and down flavoured quark distributions polarised parallel ($\uparrow$) and antiparallel ($\downarrow$) to the target proton and ΔC_{NS} and C_{NS} denote the spin-dependent and spin-independent perturbative QCD coefficients [30].

In Fig. 2 we show the SLAC data on $g_1^{(p-n)}(x)$ together with the NMC measurement [31] of $F_2^{(p-n)}(x)$ at $Q^2 = 4\text{GeV}^2$. The NMC parametrised their small x data using the fit:

$$(F_2^p - F_2^n) \sim (0.20 \pm 0.03)x^{0.59 \pm 0.06} \quad \text{at } (0.004 < x < 0.15). \tag{11}$$

The data in Fig. 2 clearly exhibits the inequality

$$2x(g_1^p - g_1^n) > (F_2^p - F_2^n) \quad \text{at } (0.01 < x < 0.12). \tag{12}$$

The inequality (12) persists in the deep inelastic data up to $x \sim 0.4$. Recent measurements from SMC [32] are consistent with (12) down to $x \sim 0.005$.[2]

The ratio of the polarised to unpolarised structure function data in Fig. 2 is roughly constant $2xg_1^{(p-n)}/F_2^{(p-n)} \simeq 1.7$ over the small x range $(0.01 < x < 0.12)$. Keeping in mind that one does not normally expect the constituent quark model to describe small x physics, it is interesting to observe that the ratio of the measured structure functions $2xg_1^{p-n}/F_2^{p-n} \simeq 1.7$ is consistent with the simple SU(6) prediction $2xg_1^{p-n}/F_2^{p-n} = \frac{5}{3}$ in the x range $0.01 < x < 0.12$. (The ratio $2xg_1^{(p-n)}/F_2^{(p-n)} \simeq \frac{5}{3}$ persists in the data up until $x \simeq 0.2$. At larger x it slowly decreases towards unity as the structure functions $2xg_1^{(p-n)}$ and $F_2^{(p-n)}$ fall away to zero when x approaches one [33] – consistent with the prediction of QCD counting rules.)

If Regge theory (with $\alpha_{a_1} = -0.4$) does work at $Q^2 = 0$, then we expect the protoproduction cross-sections to behave as $(\sigma_A - \sigma_P)^{(p-n)} \sim s_{\gamma p}^{-1.4}$ and $(\sigma_A + \sigma_P)^{(p-n)} \sim s_{\gamma p}^{-0.5}$ when $s_{\gamma p}$ becomes large (greater than a few GeV^2). Regge theory predicts that $(\sigma_A - \sigma_P)^{(p-n)} < (\sigma_A + \sigma_P)^{(p-n)}$ when $s_{\gamma p} \to \infty$. If the Regge predictions are valid for low Q^2, then we expect the inequality (12) to reverse at some Q_0^2 between photoproduction and deep inelastic Q^2. This can be checked in future experiments at CEBAF and HERA.

4 A first estimate of the high-energy part of the DHG integral

4.1 g_1 at low Q^2

The SLAC E-143 [34] and SMC [9,32] experiments have measured the spin asymmetry

$$A_1 = \frac{\sigma_A - \sigma_P}{\sigma_A + \sigma_P} \tag{13}$$

for both proton and deuteron targets over a wide range of Q^2, including between 0.25 GeV^2 and 0.80 GeV^2.

We list the SLAC [34] and SMC [32] low x, low Q^2 data in Table 1. This data has the following general features.

[2] The inequality (12) corresponds to the parton inequality $(d + \overline{d})^{\downarrow}(x) > (u + \overline{u})^{\downarrow}(x)$. This parton inequality holds both at leading order and also at next-to-leading order. The coefficients C_{NS} and ΔC_{NS} have the perturbative expansion $\delta(1-x) + \frac{\alpha_s}{2\pi} f(x)$. They are related (in the $\overline{\text{MS}}$ scheme) by [30] $\Delta C_{NS}(x) = C_{NS}(x) - \frac{\alpha_s}{2\pi}\frac{4}{3}(1+x)$. Since the coefficient C_{NS} is greater than ΔC_{NS} at next-to-leading order, it follows that the parton-model inequality $(d + \overline{d})^{\downarrow}(x) > (u + \overline{u})^{\downarrow}(x)$ is more pronounced at next-to-leading order than at leading order

Table 1. Small Q^2 data from E-143 and SMC

x	Q^2	$s_{\gamma p}$	A_1^p	A_1^d
SLAC E-143				
0.035	0.32	9.7	0.053 ± 0.030	-0.020 ± 0.032
0.035	0.65	18.8	0.069 ± 0.018	$+0.039 \pm 0.046$
0.050	0.37	7.9	0.110 ± 0.033	$+0.004 \pm 0.034$
0.050	0.79	15.9	0.117 ± 0.019	$+0.023 \pm 0.034$
0.080	0.42	5.7	0.095 ± 0.037	$+0.031 \pm 0.040$
0.080	0.71	9.0	0.129 ± 0.038	-0.010 ± 0.043
0.125	0.47	4.2	0.110 ± 0.048	$+0.022 \pm 0.057$
CERN SMC				
0.0009	0.25	278	-0.024 ± 0.037	-0.067 ± 0.040
0.0011	0.30	273	-0.024 ± 0.043	$+0.052 \pm 0.046$
0.0011	0.34	309	$+0.060 \pm 0.051$	$+0.046 \pm 0.052$
0.0014	0.38	272	$+0.054 \pm 0.028$	-0.028 ± 0.032
0.0017	0.46	271	$+0.048 \pm 0.033$	-0.069 ± 0.037
0.0019	0.55	290	-0.060 ± 0.034	$+0.052 \pm 0.037$
0.0023	0.59	257	$+0.004 \pm 0.029$	$+0.076 \pm 0.035$
0.0025	0.70	280	$+0.030 \pm 0.030$	-0.043 ± 0.035

First, the isoscalar deuteron asymmetry A_1^d is very small and consistent with zero in both the E-143 and SMC low Q^2 bins. Second, there is a clear positive proton asymmetry in the E-143 data, signalling a strong isotriplet term in $(\sigma_A - \sigma_P)$ at $\sqrt{s_{\gamma p}} \simeq 3.5$GeV. At higher $\sqrt{s_{\gamma p}} \simeq 16.7$GeV, the combined SMC A_1^p data is consistent with zero. Further data will come from the forthcoming HERMES measurements of g_1 at low x and low Q^2 with $\sqrt{s_{\gamma p}} \simeq 7$GeV.

Due to the wide separation in $s_{\gamma p}$ range measured in E-143 and SMC, we combine the low Q^2 data to obtain one point corresponding to each experiment. This is shown in Table 2. We make two cuts:

1. keeping $\sqrt{s_{\gamma p}} \geq 2.5$GeV to ensure that our data set is well beyond the resonance region and including all such data that the mean Q^2 is kept below 0.5GeV^2 for each experiment. (In practice, this amounts to a common Q^2 cut of 0.7GeV^2 and yields a mean $Q^2 = 0.45$GeV^2 for each experiment.)
2. including all data at $\sqrt{s_{\gamma p}} \geq 2$GeV and $Q^2 \leq 0.8$GeV^2.

In what follows, we work with Cut (a). This choice of cut is a compromise between keeping Q^2 as low as possible and including the maximum amount of data. The choice $Q^2_{\max} \simeq 0.5$GeV^2 is motivated by the HERA data [35,36] on $(\sigma_A + \sigma_P)$ which rises with increasing $\sqrt{s_{\gamma p}}$ according to soft Regge theory up to $Q^2 \simeq 0.5$GeV^2. At larger Q^2 the HERA data exhibits evidence of Q^2 dependence in the effective Regge intercepts for high-energy, virtual photoabsorption. The low Q^2 asymmetry measurements in Table 1 show no clear Q^2 dependence in either experiment.

To make a first estimate of the spin asymmetry at $Q^2 = 0$ we shall assume that the large $\sqrt{s_{\gamma p}}$ A_1 is approximately independent of Q^2 between $Q^2 = 0$ and $Q^2 \simeq 0.5$ GeV^2. Since the E-143 data at lower $\sqrt{s_{\gamma p}}$ exhibits a clear positive signal in A_1^p at low Q^2 we choose to normalise

Table 2. A_1 at large $s_{\gamma p}$ and low Q^2

Cuts	$\langle Q^2 \rangle$	$s_{\gamma p}$	A_1^p	A_1^d
(a) $\langle Q^2 \rangle \leq 0.5\mathrm{GeV}^2$, $s_{\gamma p} \geq 7\mathrm{GeV}^2$				
	0.45	12	0.077 ± 0.016	$+0.008 \pm 0.022$
	0.45	279	0.011 ± 0.013	$+0.002 \pm 0.014$
(b) $Q^2 \leq 0.8\mathrm{GeV}^2$, $s_{\gamma p} \geq 4\mathrm{GeV}^2$				
	0.53	10	0.098 ± 0.013	$+0.016 \pm 0.016$
	0.45	279	0.011 ± 0.013	$+0.002 \pm 0.014$

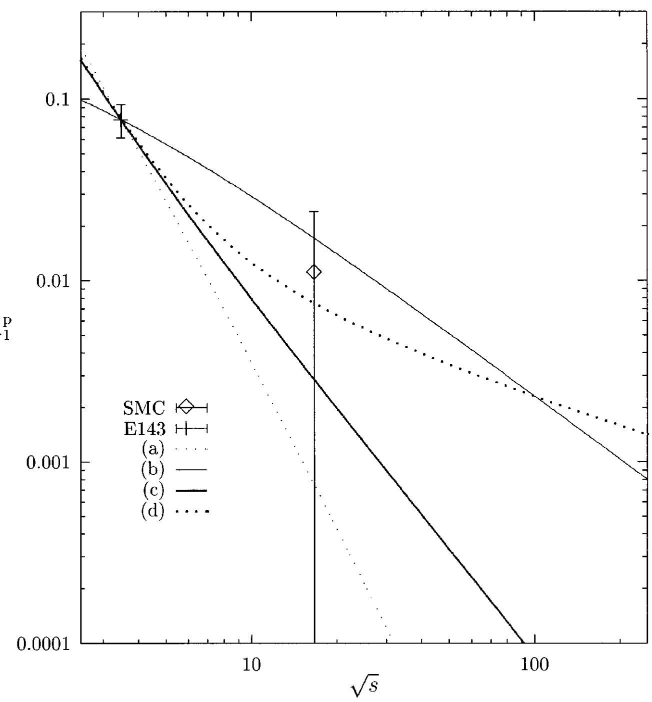

Fig. 3. The real photon asymmetry A_1^p as a function of $\sqrt{s}$ for different Regge behaviours for $(\sigma_A - \sigma_P)$: given entirely by (1a) the (a_1, f_1) terms in (2) with Regge intercept either $-\frac{1}{2}$ (conventional) or (1b) $+\frac{1}{2}$; (2) by 2/3 isovector (conventional) a_1 and 1/3 two non-perturbative gluon exchange contributions at $\sqrt{s} = 3.5\mathrm{GeV}$; (3) by 2/3 isovector (conventional) a_1 and 1/3 pomeron-pomeron cut contributions at $\sqrt{s} = 3.5\mathrm{GeV}$

to E-143. For the total photoproduction cross-section we take

$$(\sigma_A + \sigma_P) = 67.7 s_{\gamma p}^{+0.0808} + 129 s_{\gamma p}^{-0.4545} \quad (14)$$

(in units of μb), which is known to provide a good Regge fit for $\sqrt{s_{\gamma p}}$ between 2.5GeV and 250GeV [37]. (Here, the $s_{\gamma p}^{+0.0808}$ contribution is associated with pomeron exchange and the $s_{\gamma p}^{-0.4545}$ contribution is associated with the isoscalar ω and isovector ρ trajectories.) Multiplying A_1^p by the value of $(\sigma_A + \sigma_P)$ at $\sqrt{s_{\gamma p}} = 3.5\mathrm{GeV}$, we make a first estimate

$$(\sigma_A - \sigma_P) \simeq +10\mu\mathrm{b} \ \text{at} \ (Q^2 = 0, \sqrt{s_{\gamma p}} = 3.5\mathrm{GeV}). \quad (15)$$

The small isoscalar deuteron asymmetry A_1^d indicates that the isoscalar contribution to A_1^p in the E-143 data is unlikely to be more than 30%. In Fig. 3 we show the asymmetry A_1^p as a function of $\sqrt{s_{\gamma p}}$ between 2.5 and 250 GeV for the four different would-be Regge behaviours for $(\sigma_A - \sigma_P)$: that the high energy behaviour of $(\sigma_A - \sigma_P)$ is given

1. entirely by the (a_1, f_1) terms in (4,5) with Regge intercept either (1) $-\frac{1}{2}$ (conventional) or (2) $+\frac{1}{2}$ (motivated by the observed small x behaviour of $g_1^{(p-n)}$ in deep inelastic scattering),
2. by taking 2/3 isovector (conventional) a_1 and 1/3 two non-perturbative gluon exchange contributions at $\sqrt{s} = 3.5\mathrm{GeV}$,
3. by taking 2/3 isovector (conventional) a_1 and 1/3 pomeron-pomeron cut contributions at $\sqrt{s_{\gamma p}} = 3.5\mathrm{GeV}$.

(In Fig. 3 we take the mass parameter in the Regge fit, (5), as $\mu^2 = 0.5\mathrm{GeV}^2$.) The SMC low x, low Q^2 data are consistent with each of the four curves in Fig. 3. If the polarised proton beam option is realised at HERA, it will be possible to measure A_1^p to an accuracy of 0.0003 at $\sqrt{s_{\gamma p}}$ between 50 and 250 GeV assuming an integrated luminosity $\mathcal{L} \simeq 500\mathrm{pb}^{-1}$ [38].

4.2 The high-energy part of the (DHG) integral

We now estimate the high-energy part of the Drell-Hearn-Gerasimov sum-rule using low Q^2 Regge theory. Since $(\sigma_A - \sigma_P)$ in (15) is predominantly isotriplet we first fit a Regge form $(\sigma_A - \sigma_P) \sim s_{\gamma p}^{\alpha - 1}$ through the value $(\sigma_A - \sigma_P) = +10\mu$b in (15) and allow α to vary between $-\frac{1}{2}$ and $+\frac{1}{2}$. This range of α is motivated by our discussion of the Q^2 dependence of g_1 in Sect. 3.1. We believe that it represents a generous variation over the range of possible values for α_{a_1} and α_{f_1} in the Regge formulae (4,5). Taking into account the error on the E-143 measurement of A_1^p, we estimate $+25 \pm 10\mu$b for the high-energy ($\sqrt{s_{\gamma p}} \geq 2.5\mathrm{GeV}$) contribution to the Drell-Hearn-Gerasimov sum-rule for a proton target. This is about 10% of the sum-rule.

We consider other possible Regge contributions to $(\sigma_A - \sigma_P)$. Any two-pomeron cut contribution to $(\sigma_A - \sigma_P)$ decays more slowly with increasing $s_{\gamma p}$ than the other possible Regge contributions in (4,5). Consider the scenario where the value of $(\sigma_A - \sigma_P)$ in (15) is made up of a 1/3 isoscalar two-pomeron cut and 2/3 combination of a_1 and f_1 contributions. The high-energy

($\sqrt{s_{\gamma p}} \geq 2.5$GeV) part of the Drell-Hearn-Gerasimov sum-rule becomes $+26 \pm 5\mu$b if we use the "conventional" value ($\alpha = -\frac{1}{2}$) for the intercept of the a_1 and f_1 trajectories and $+33 \pm 7\mu$b if we use the "exotic" value ($\alpha = +\frac{1}{2}$). We believe that the 1/3 two-pomeron cut scenario gives a reasonable upper bound on the isosinglet contribution to (15) because of the small deuteron asymmetries in Table 2 and because there is no evidence for any two-pomeron cut contribution in the high Q^2 polarised deep inelastic data [9]. (A two-pomeron cut contribution would lead to a sharp rise in the absolute value of $g_1^{(p+n)}$ at small x.) The "conventional" a_1 scenario is consistent with our preferred estimate $+25 \pm 10\mu$b whereas the two-pomeron cut with "exotic" a_1 scenario lies at the margins of it.

Our estimate $+25 \pm 10\mu$b is intended as a guide for future experiments.

5 Conclusions

Using the SLAC data on g_1 at low x and low Q^2 we estimate that about 10% of the Drell-Hearn-Gerasimov sum-rule comes from the Regge region $\sqrt{s_{\gamma p}} > 2.5$GeV. This Regge contribution ($+25 \pm 10\mu$b) is predominantly isotriplet. It is consistent with the multipole estimates of the low-energy part of the Drell-Hearn-Gerasimov sum-rule which suggest that the isosinglet part of the (DHG) integral may be all but fully saturated by the nucleon resonances and that a $\simeq +65\mu$b contribution to the isotriplet part of the sum-rule comes from non-resonance physics. Experiments at CEBAF, ELSA, GRAAL, LEGS and MAMI will measure the low and medium energy contributions to the (DHG) integral up to $\sqrt{s_{\gamma p}} \simeq 3.5$GeV. High-energy polarised photon beams would enable these measurements to be continued into the Regge region and to make a more accurate test of the Drell-Hearn-Gerasimov sum-rule.

Spin dependent Regge theory makes a prediction for the high-energy part of $(\sigma_A - \sigma_P)$ at $Q^2 = 0$. It is presently unknown how high in Q^2 this Regge behaviour is supposed to apply. Certainly, it does not provide a good description of $g_1^{(p-n)}$ at deep inelastic Q^2 where $g_1^{(p-n)} \sim x^{-0.5}$ in contrast with the naive Regge prediction $g_1^{(p-n)} \sim x^{+0.4}$. Some insight may come from the CEBAF experiment E-97-003 [39] which will make a precision measurement of the Q^2 dependence of the Regge onset in $(\sigma_A - \sigma_P)$ at $\sqrt{s_{\gamma p}} \sim 3.5$GeV between Q^2 of 0.02 and 0.5 GeV^2 and from the HERMES low Q^2 data.

It is a pleasure to thank N. Bianchi, A. Brüll, J-P. Chen, A. De Roeck, E. De Sanctis, G. Garvey, M. Glück, T. Goldman, P.V. Landshoff, G. Rädel, E. Reya and A.W. Thomas for helpful discussions about g_1 and DHG physics. Support from the Alexander von Humboldt Foundation (SDB) and the U.S. Department of Energy (MMB) is gratefully acknowledged.

References

1. S.D. Drell and A.C. Hearn, Phys. Rev. Lett. **162** (1966) 1520; S.B. Gerasimov, Yad. Fiz. **2** (1965) 839
2. J.D. Bjorken, Phys. Rev. **148** (1966) 1467; Phys. Rev. **D1** (1970) 1376
3. J. Ellis and R.L. Jaffe, Phys. Rev. **D9** (1974) 1444; (E) **D10** (1974) 1669
4. S. D. Bass, Mod. Phys. Lett. **A12** (1997) 1051
5. D. Drechsel, Prog. Part. Nucl. Phys. **34** (1995) 181
6. J. Kodaira, Nucl. Phys. **B165** (1980) 129
7. S.A. Larin, Phys. Lett. **B334** (1994) 192; **404** (1997) 153
8. EMC Collaboration (J Ashman et al.) Phys. Lett. **B206** (1988) 364; Nucl. Phys. **B328** (1989) 1
9. The Spin Muon Collaboration (D. Adams et al.), Phys. Lett. **B396** (1997) 338; (B. Adeva et al.), Phys. Lett. **B412** (1997) 414
10. The HERMES Collaboration (K. Ackerstaff et al.), Phys. Lett. **B404** (1997) 383
11. The E-143 Collaboration (K. Abe et al.), Phys. Rev. Lett. **74** (1995) 346
12. The E-154 Collaboration (K. Abe et al.), Phys. Rev. Lett. **79** (1997) 26
13. H.-Y. Cheng, Int. J. Mod. Phys. **A11** (1996) 5109; M. Anselmino, A. Efremov and E. Leader, Phys. Rept. **261** (1995) 1
14. I. Karliner, Phys. Rev. **D7** (1973) 2717; R.L. Workman and R.A. Arndt, Phys. Rev. **D45** (1992) 1789; A.M. Sandorfi, C.S. Whisnant and M. Khandaker, Phys. Rev. **D50** (1994) R6681
15. M. Anselmino, E. Leader and B.L. Ioffe, Yad. Fiz. **49** (1989) 214
16. H.W. Hammer, D. Drechsel and T. Mart, nucl-th/9701008 (1997)
17. R.L. Heimann, Nucl. Phys. **B64** (1973) 429
18. J. Ellis and M. Karliner, Phys. Lett. **B213** (1988) 73
19. F.E. Close and R.G. Roberts, Phys. Lett. **B336** (1994) 257
20. L. Galfi, J. Kuti and A. Patkos, Phys. Lett. **B31** (1970) 465; F.E. Close and R.G. Roberts, Phys. Rev. Lett. **60** (1988) 1471
21. S.D. Bass and P.V. Landshoff, Phys. Lett. **B336** (1994) 537; P.V. Landshoff and O. Nachtmann, Z Physik **C35** (1987) 405
22. C. Young, *in* Proc. Workshop on *Deep Inelastic Scattering off Polarized Targets: Theory meets Experiment*, DESY-Zeuthen 1997, eds. J. Blümlein et al. (DESY report 97-200, 1997)
23. J. Soffer and O.V. Teryaev, Phys.Rev. **D56** (1997) 1549
24. G. Altarelli, R.D. Ball, S. Forte and G. Ridolfi, Nucl. Phys. **B496** (1997) 337
25. Various contributions *in* Proc. Workshop on *Deep Inelastic Scattering off Polarized Targets: Theory meets Experiment*, DESY-Zeuthen 1997, eds. J. Blümlein et al. (DESY report 97-200, 1997)
26. The E-154 Collaboration (K. Abe et al.), Phys. Lett. **B405** (1997) 180; The SMC Collaboration (B. Adeva et al.), CERN preprint CERN-EP-98-086 (1998)
27. M. Gluck, E. Reya, M. Stratmann and W. Vogelsang, Phys. Rev. **D53** (1996) 4775
28. T. Gehrmann and W.J. Stirling, Phys. Rev. **D53** (1996) 6100; M. Stratmann, hep-ph/9710379; D. de Florian, O.A. Samapayo and R. Sassot, Phys. Rev **D57** (1998) 5803; L.E. Gordon, M. Goshtasbpour and G.P. Ramsey, hep-

ph/9803351; E. Leader, A.V. Sidorov and D.B. Stamenov, hep-ph/9808248
29. B. Badełek and J. Kwieciński, Phys. Lett. **B418** (1998) 229
30. P. Ratcliffe, Nucl. Phys. **B223** (1983) 45
31. The New Muon Collaboration (M. Arneodo et al.), Phys. Rev. **D50** (1994) R1
32. The SMC Collaboration (B. Adeva et al.), CERN preprint EP-98-085 (1998)
33. S.D. Bass, in preparation
34. The E-143 Collaboration (K. Abe et al.), Phys. Lett. **B364** (1995) 61
35. The H1 Collaboration (C. Adloff et al.), Nucl. Phys. **B497** (1997) 3
36. The ZEUS Collaboration (J. Breitweg et al.), Phys. Lett. **B407** (1997) 432
37. A. Donnachie and P.V. Landshoff, Z Physik **C61** (1994) 139
38. S.D. Bass, M.M. Brisudová and A. De Roeck, hep-ph/9710518 (1997), *in* Proc. Workshop on *Physics with Polarized Protons at HERA*, eds. J. Blümlein et al. (DESY report 97-200, 1997)
39. TJNAF experiment E-97-003, J-P. Chen et al